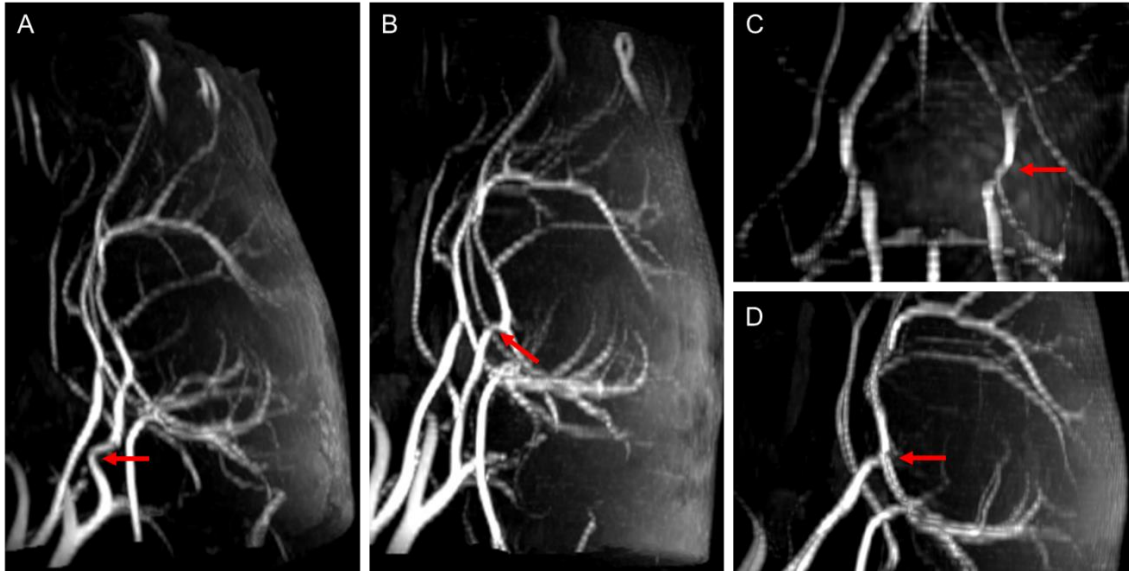
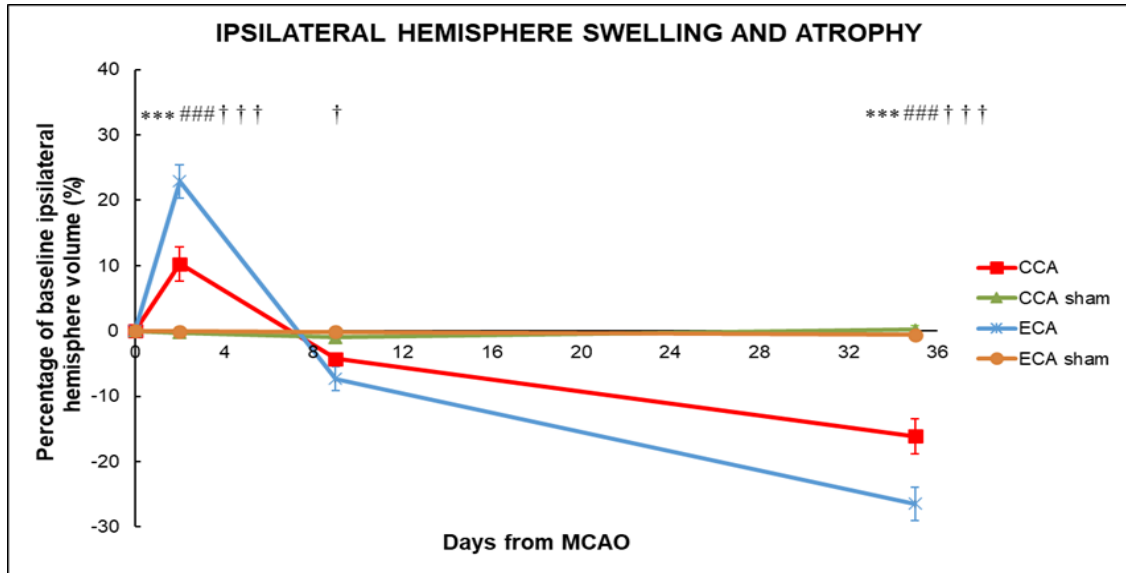


Supplementary Figure 1.



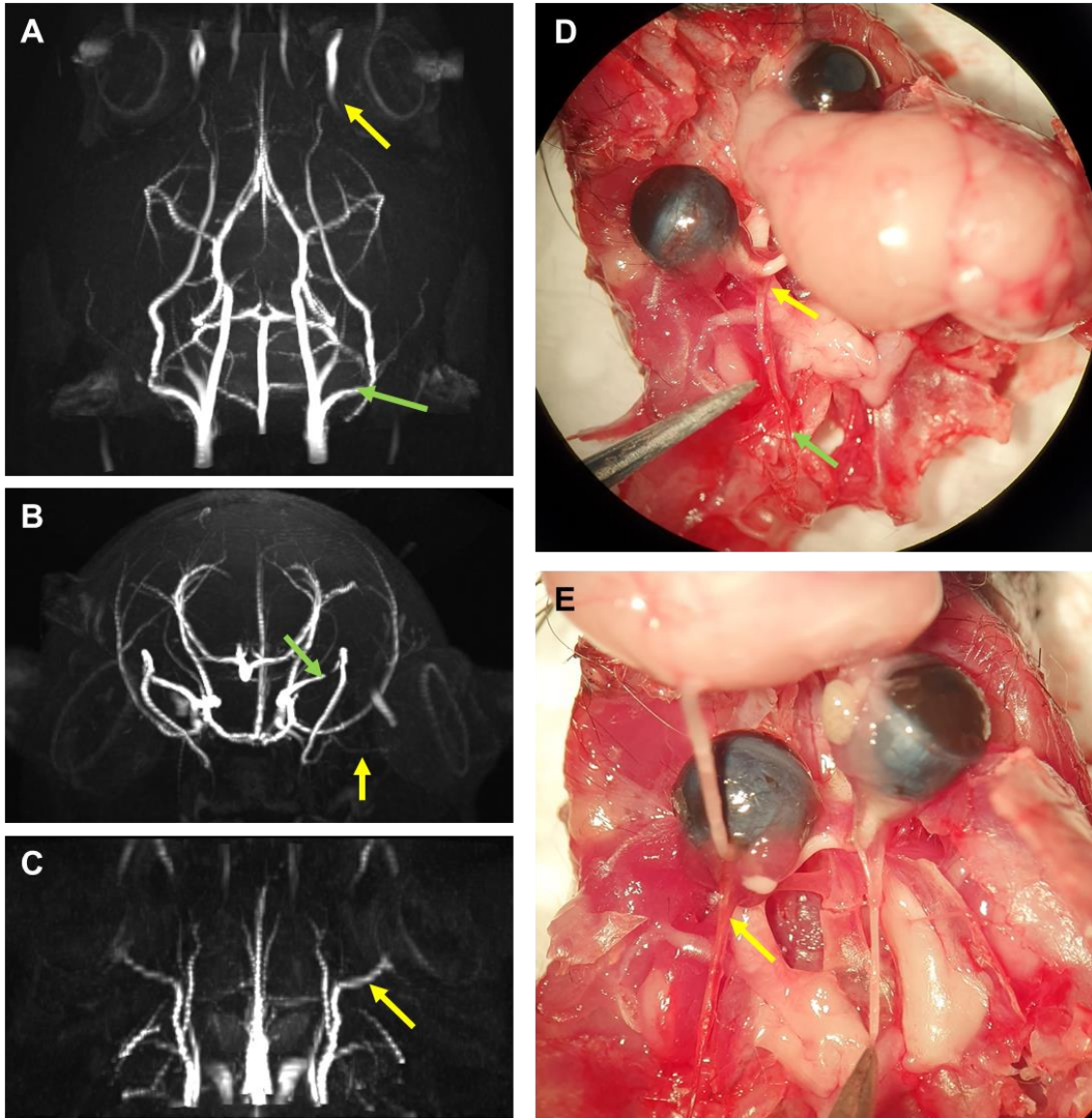
Supplementary Figure 1. High-resolution MR angiography maximum intensity projections (MIP) of healthy mouse brains show tortuosity of the ipsilateral internal carotid artery (A), S-shaped distal portion of the internal carotid artery (B) and looping of the posterior cerebral artery (C and D) altering the path of filament insertion. Red arrows represent arterial tortuosity and path alteration.

Supplementary Figure 2.



Supplementary Figure 2. The Longa (ECA) middle cerebral artery occlusion method exacerbates ipsilateral hemisphere swelling in the acute phase and tissue atrophy in the chronic phase. Ipsilateral hemisphere swelling and tissue atrophy after middle cerebral artery occlusion (MCAO) by filament insertion through the common carotid artery (CCA), external carotid artery (ECA), and in sham-operated (CCA sham and ECA sham) animals measured before (baseline - BL) and on day 2 (D2), 9 (D9), and 35 (D35) after MCAO. Statistical differences using mixed model ANOVA and Tukey post hoc test: the CCA to ECA group (***) $P < 0.0001$; CCA to CCA sham group: (###) $P < 0.0001$; ECA to ECA sham group (†††) $P < 0.0001$, (†) $P < 0.05$.

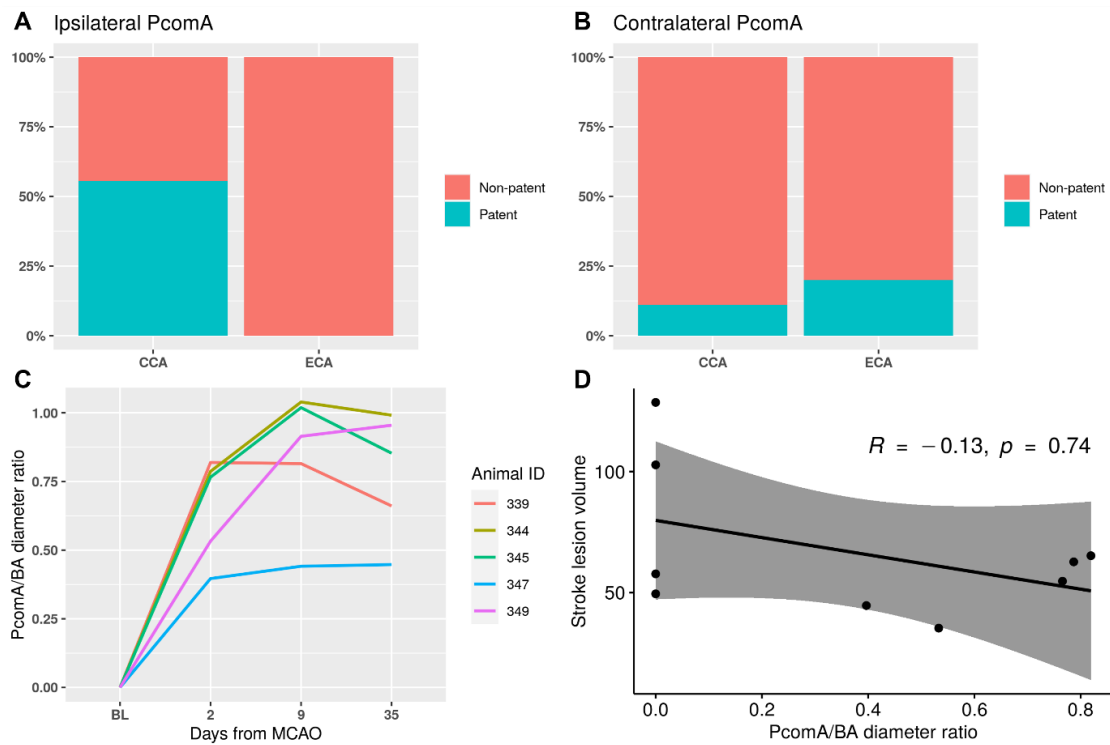
Supplementary Figure 3.



Supplementary Figure 3. High-resolution MR angiography and gross anatomical findings of the pterygopalatine artery and ophthalmic artery. Maximum intensity projections (MIP) of pre-surgery mouse brain MR angiography scans in the (A) horizontal

and (B) frontal plain show the ophthalmic artery (yellow arrow) originating from the pterygopalatine artery (green arrow). (C) MIP of the anterior part of the brain shows the ophthalmic artery (yellow arrow). The low (D) and high (E) magnification power photographs of excised mouse brain vasculature confirm the MR angiographic findings of the ophthalmic artery (yellow arrow) originating from the pterygopalatine artery (green arrow). These findings were uniform in all the experimental animals in our study.

Supplementary Figure 4.



Supplementary Figure 4. Differences in PcomA recruitment in the Koizumi (CCA) and Longa (ECA) middle cerebral artery occlusion models. (A) Analysis of the recruitment of the ipsilateral (IL) posterior communicating artery (PcomA) 2 days after middle cerebral artery occlusion (MCAO) by filament insertion through the common carotid artery (CCA) and external carotid artery (ECA) shows patent IL PcomA in 5 out of 9 animals only in the CCA ischemia-with-hypoperfusion model, in contrast to the non-patent IL PcomA in the ECA ischemia-reperfusion model. Pearson's Chi-squared test with Yates' continuity correction shows significant differences between groups ($P=0.0261$).

(B) No difference in contralateral PcomA patency 2 days after MCAO in the CCA and ECA groups. (C) Progressive increase in the PcomA patency in the Koizumi (CCA) group from the acute phase (day 2) toward the subacute phase (day 9), with gradual decrease toward the chronic phase of ischemia (day 35). Note that none of the animals had detectable IL PcomA patency at baseline. (D) Nonsignificant low negative correlation of PcomA size and lesion volume 2 days after Koizumi (CCA) MCAO (Spearman rank-order correlation coefficient $R=-0.13$, $P=0.74$; $n=9$). The size of the posterior communicating artery (PcomA) was measured manually (in each time point in 3 repetitions) as a ratio of PcomA diameter to basilar artery (BA) diameter on maximum intensity projections of raw 3D-TOF images based on previously described methods^{28,29}.